J. Electrochem. Sci. Eng. **13(6)** (2023) S11-S23

Open Access : : ISSN 1847-9286
www.jESE-online.org

Supplementary material to

Primary aluminum-air flow battery for high-power applications: Optimization of power and self-discharge

Dayatri Bolaños-Picado[1,2], Cindy Torres[1,3] and Diego González-Flores[2,3,4,✉]

[1]*Departamento de Ingeniería Química, 11501 2060, Sabanilla de Montes de Oca, San José, Costa Rica*
[2]*Centro de Electroquímica y Energía Química (CELEQ), Universidad de Costa Rica, 11501 2060, Sabanilla de Montes de Oca, San José, Costa Rica*
[3]*Centro de Investigación en Ciencia e Ingeniería de Materiales (CICIMA), 11501 2060, Sabanilla de Montes de Oca, San José, Costa Rica*
[4]*Escuela de Química, Universidad de Costa Rica, 11501 2060, San Pedro de Montes de Oca, San José, Costa Rica*

J. Electrochem. Sci. Eng. ***13(6)*** *(2023) 895-909* http://dx.doi.org/10.5599/jese.2075

Unit cell design

In Figure S-1, the dynamic characteristics of the electrolyte flow for the first and the last models are shown. Through image processing, it was determined that in the first model 31 % of the anode surface was not effectively exposed to the circulating electrolyte. That percentage was reduced to 17 % in the last model. Effective electrolyte exchange is important because the larger the anode area in contact with a fresh electrolyte, the better the cell performance [1].

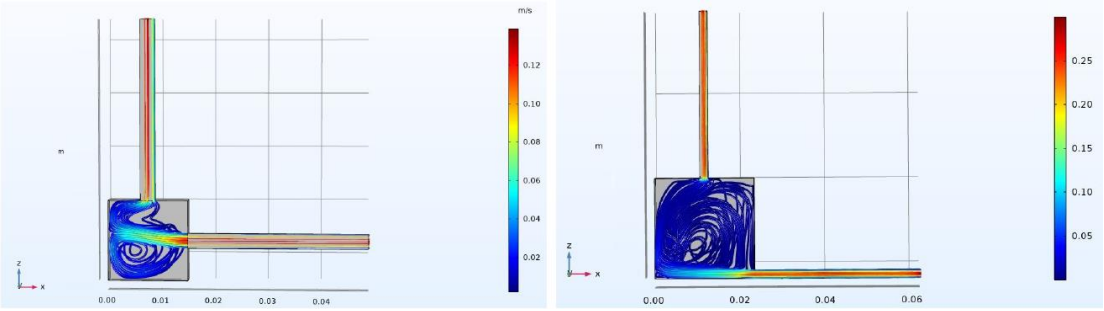

Figure S-1. *Electrolyte domain simulation in COMSOL Multiphysics 5.5*

The first unit cell consisted of three structures, one for each battery component. Figure S-2 shows the construction plan with the following color coding: blue for the cathode, green for the electrolyte, and red for the anode. Each main piece was designed with a square geometry, with 6.38 cm per side. Once assembled, the total thickness of the cell was 1.13 cm, of which 0.57 cm corresponded to the electrolytic structure.

In the cathode structure, the membrane must be glued on the inside of the cell, since this coincides with the face of the membrane that has a suitable material to carry out the union; the opposite side of the membrane has a thin film of carbon which is peeled off with prolonged cell operation and may become a leak point.

Two conduits were made in the electrolytic structure to allow the flow of the solution, and the electrolyte flows upwards within the cell to ensure the correct filling of the entire space. We aimed for the smallest practical thickness, considering that the space between the electrodes must constitute a space large enough to avoid a short circuit, but as small as possible to minimize the distance the ions travel [2]. This last aspect aims to minimize ohmic polarization, which negatively affects the voltage delivered by the cell.

The anode structure was designed to fit the exact size of the aluminum plate, which allowed controlling of the anode area exposed to the electrolyte.

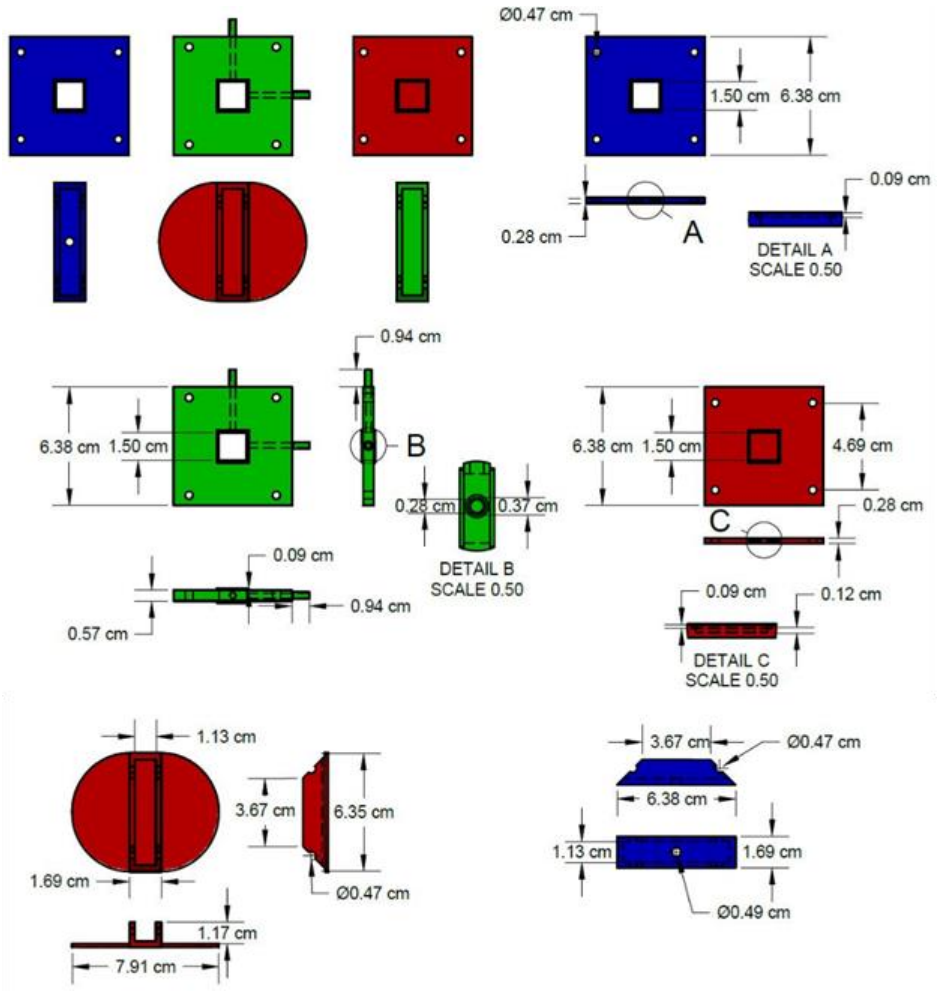

Figure S-2. *Construction plan of the first unit cell prototype*

Figure S-3 shows our current model in which the anodic and electrolytic structures were fused into one piece. This allowed solving the problem present since the second model, which is related to the complexity of contacting the cathode. Since the structure had a greater thickness, it allowed the creation of the exit channel with a better alignment.

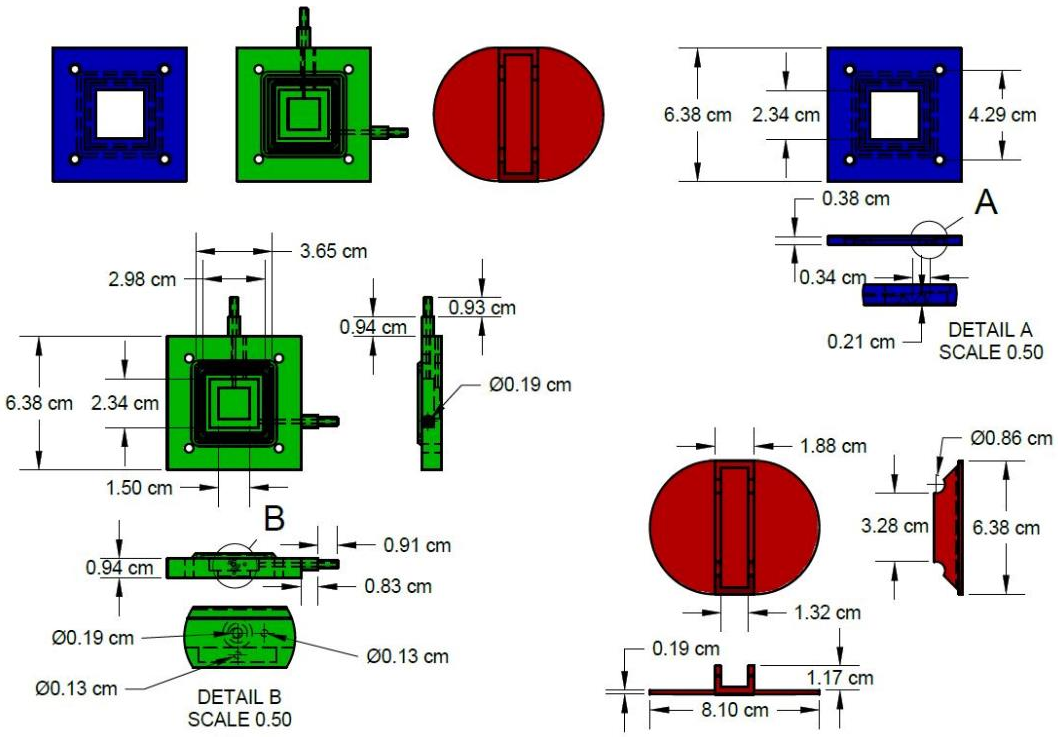

Figure S-3. *Construction plan of the unit cell*

Evaluation of the recirculation system in the operation of unit cell

To determine if there is a significant difference in the operating time of the cell when the electrolyte is in circulation or not, a Student's T-test was performed with unequal variances in the case of 4 mol L^{-1} KOH and a Student's *T*-test with equal variances in the case of 4 mol L^{-1} KOH + 1 mol L^{-1} NH_4VO_3 (See Table S-1).

Table S-1*. Student's T-test results for cell discharge time data obtained with and without electrolyte recirculation*

Battery system	*T* (Student's *T*-test)	*p*-value
4 mol L^{-1} KOH	3.33	0.04
4 mol L^{-1} KOH + 1 mol L^{-1} NH_4VO_3	35.45	1.89×10^{-6}

Through *p*-value, it can be concluded with 95 % confidence that the operating time when the cell has the electrolyte in circulation is significantly higher.

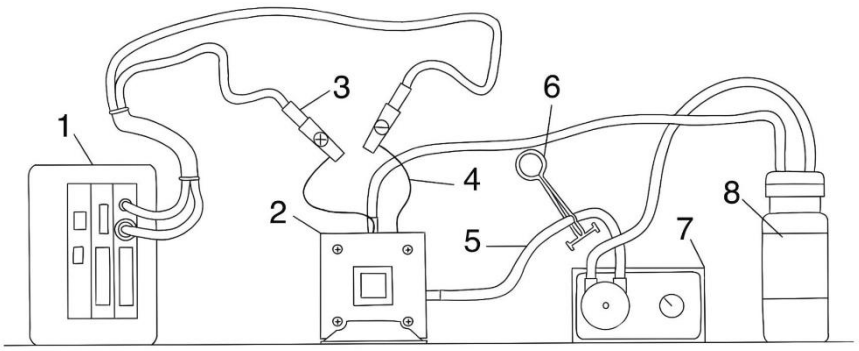

1 Power supply, 2 Unit cell, 3 Connectors, 4 Electrodes, 5 Hose,
6 Mohr's pinch clamp, 7 Peristaltic pump, 8 Storage tank

Figure S-4. *Experimental diagram used in the construction of discharge curves without electrolyte flow*

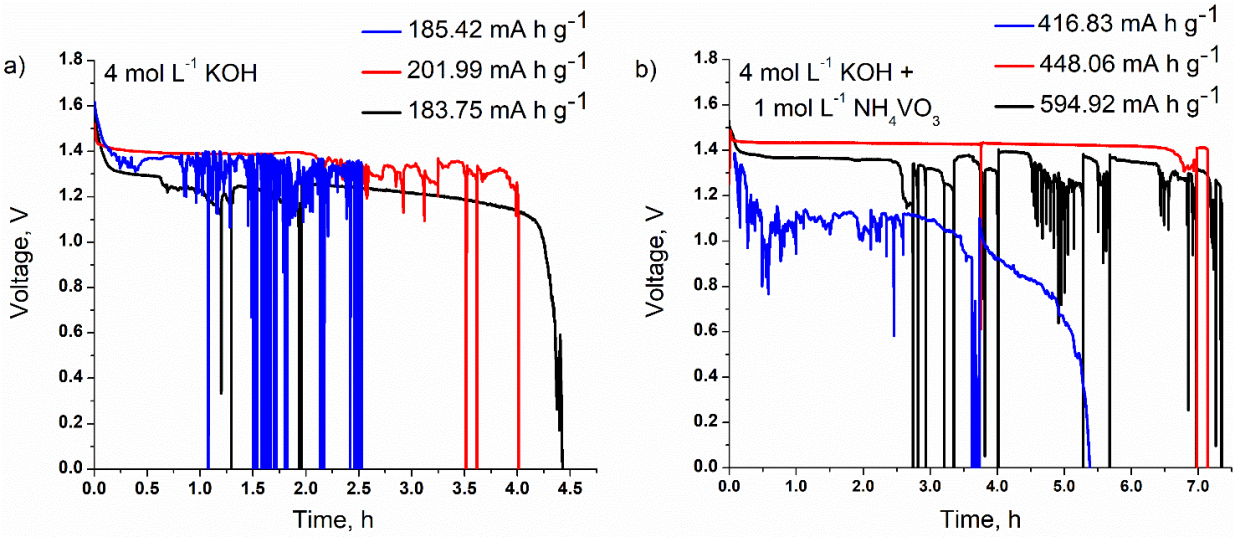

Figure S-5. *Unit cell discharge curves and capacity values obtained using a) 4 mol L^{-1} KOH and b) 4 mol L^{-1} KOH + 1 mol L^{-1} NH_4VO_3 in a system without electrolyte flow, at current density equal to 3.33 mA cm^{-2}*

Potassium hydroxide concentration evaluation

To determine if there is a significant difference in the power and current density obtained by the cell according to the concentration of the potassium hydroxide solution, a Student's *T*-test was performed with unequal variances.

Table S-2*. Student's T-test results for the power and current density data obtained by the cell according to the concentration of the potassium hydroxide solution.*

Variable	*T* (Student's *T*-test)	*p*-value
Power	13.55	2.66×10^{-3}
Current density	207.51	4.63×10^{-6}

Through *p*-value, it can be concluded with 95 % confidence that the power and current density obtained with the 4 mol L^{-1} KOH solution are significantly higher than when 0.1 mol L^{-1} KOH was used.

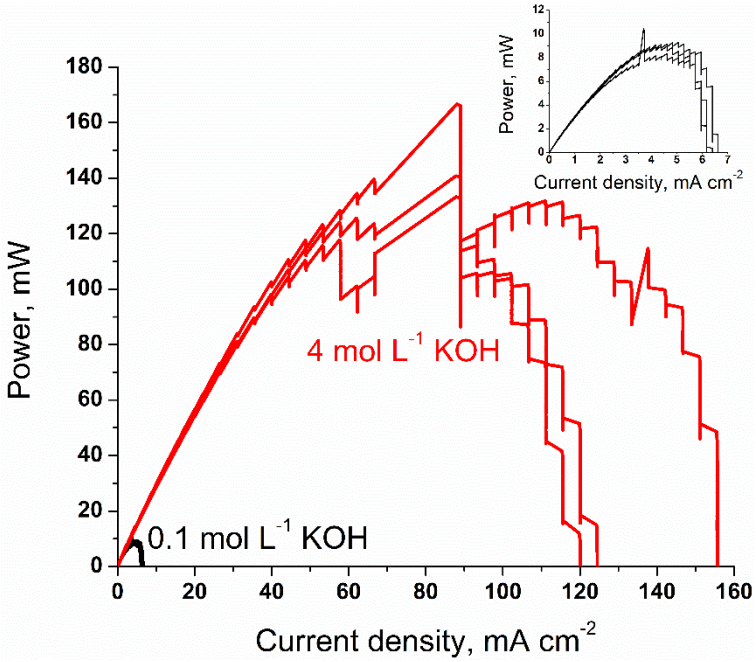

Figure S-6. *Power as a function of current density obtained with the unit cell using two concentrations of potassium hydroxide*

Evaluation of anticorrosive capacity and a ventilation system

A factorial design 2^2 was carried out whose independent variables were the use of anticorrosive and a ventilation system.

***Table S-3**. Results of the ANOVA for the determination of the conditions that maximize the power delivered by the unit cell with a current density of 3.33 mA cm^{-2}*

Source of variability	p-value
Anticorrosive (A)	0.000
Ventilation (B)	0.035
A - B	0.030

Through p-value, it is concluded with 95 % confidence that both the two effects and their interaction are significant. Since you want to maximize the response variable (power), you should not use ventilation or add an anticorrosive agent to the electrolyte.

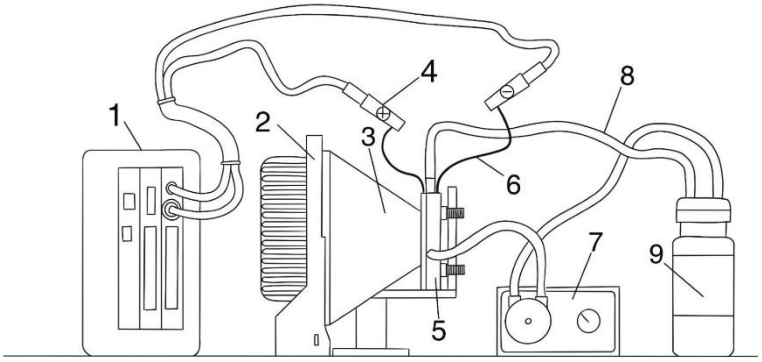

1 Power supply, 2 Fan, 3 Flow director, 4 Connectors, 5 Unit cell, 6 Electrodes, 7 Peristaltic pump, 8 Hose, 9 Storage tank

***Figure S-7.** Experimental diagram used for assisted ventilation treatments*

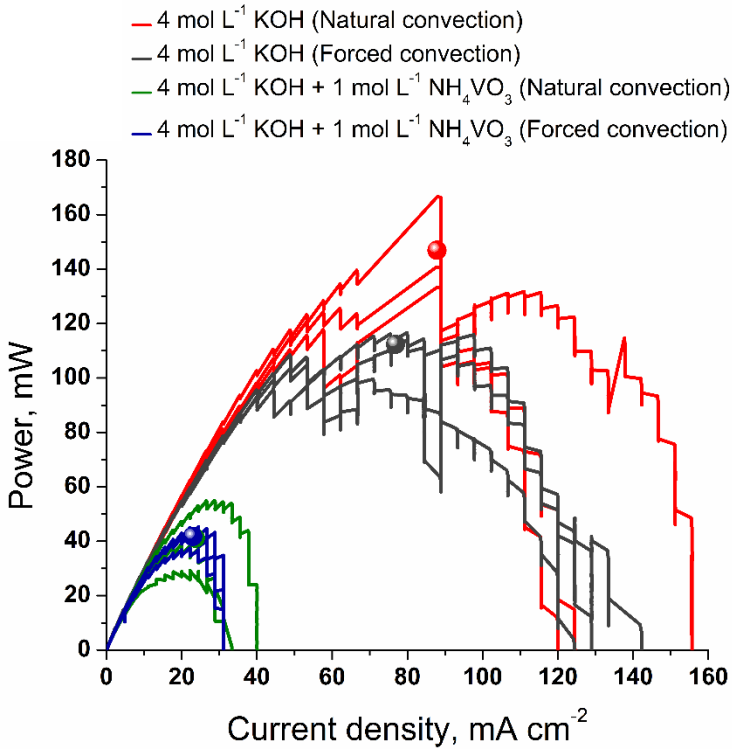

***Figure S-8.** Power obtained with the unit cell as a function of current density*

Corrosion rate test

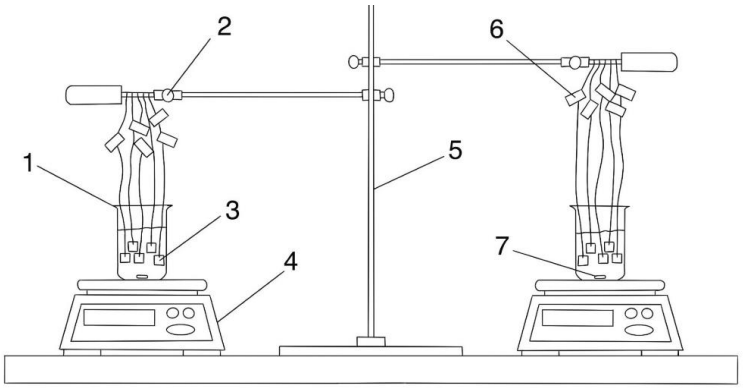

1 Beaker 250 mL, 2 Two prong utility clamps, 3 Aluminum alloy, 4 Magnetic stirrer, 5 Retort stand, 6 Tag, 7 Magnetic stirring bar

Figure S-9. *Experimental diagram for determination of corrosion rate*

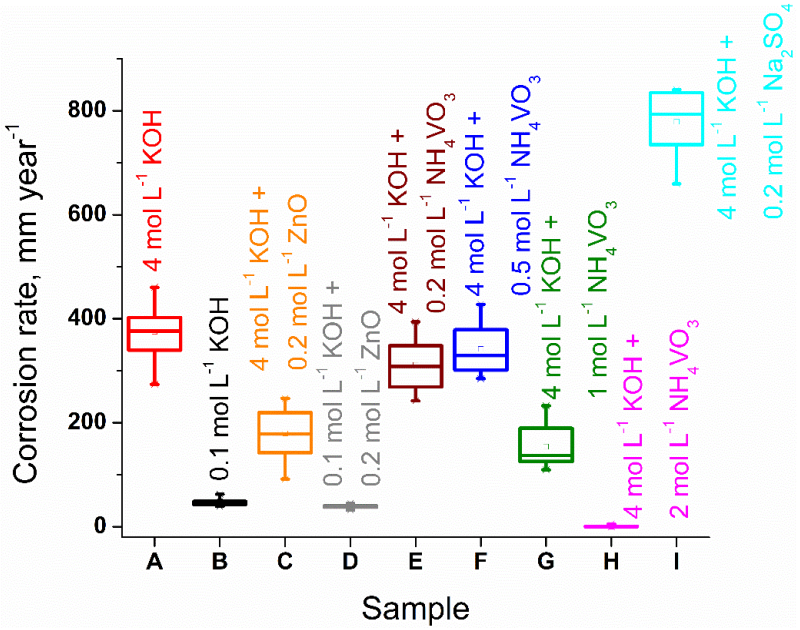

Figure S-10. *Box diagram for annual corrosion rate of 5052 aluminum A: 4 mol L^{-1} KOH, B: 0.1 mol L^{-1} KOH, C: 4 mol L^{-1} KOH + 0.2 mol L^{-1} ZnO, D: 0.1 mol L^{-1} KOH + 0.2 mol L^{-1} ZnO, E: 4 mol L^{-1} KOH + 0.2 mol L^{-1} NH_4VO_3, F: 4 mol L^{-1} KOH + 0.5 mol L^{-1} NH_4VO_3, G: 4 mol L^{-1} KOH + 1 mol L^{-1} NH_4VO_3, H: 4 mol L^{-1} KOH + 2 mol L^{-1} NH_4VO_3 and I: 4 mol L^{-1} KOH + 0.2 mol L^{-1} $Na_2SO_4·H_2O$*

Determination of anticorrosive agents

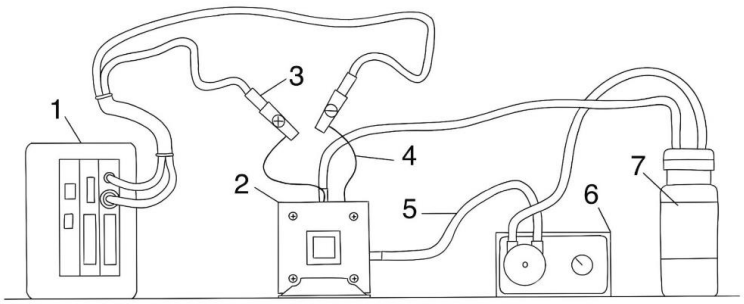

1 Power supply, 2 Unit cell, 3 Connectors, 4 Electrodes, 5 Hose, 6 Peristaltic pump, 7 Storage tank

Figure S-11. *Experimental diagram used in the construction of discharge curves*

Table S-4. *Summary of performance of different battery systems in different electrolytes*

Battery system	Current density, mA cm^{-2}	Capacity, mA h^{-1} g^{-1}
0.1 mol L^{-1} KOH	3.33	1656.99
		1756.55
		1683.62
4 mol L^{-1} KOH	0.67	18.62
		22.88
		24.56
	3.33	102.67
		109.59
		186.21
4 mol L^{-1} KOH + 0.2 mol L^{-1} NH_4VO_3	0.67	50.55
		54.76
		63.29
	3.33	46.85
		60.40
		63.12
4 mol L^{-1} KOH + 0.5 mol L^{-1} NH_4VO_3	0.67	41.80
		41.37
		40.99
	3.33	147.15
		244.92
		178.38
4 mol L^{-1} KOH + 1 mol L^{-1} NH_4VO_3	0.67	58.40
		82.16
		71.98
	3.33	653.10
		712.78
		655.68
4 mol L^{-1} KOH + 2 mol L^{-1} NH_4VO_3	0.67	2163.96
		2271.11
		2274.08
	3.33	-
4 mol L^{-1} KOH + 0.2 mol L^{-1} ZnO	0.67	50.49
		51.03
		61.77
	3.33	344.82
		355.41
		376.27

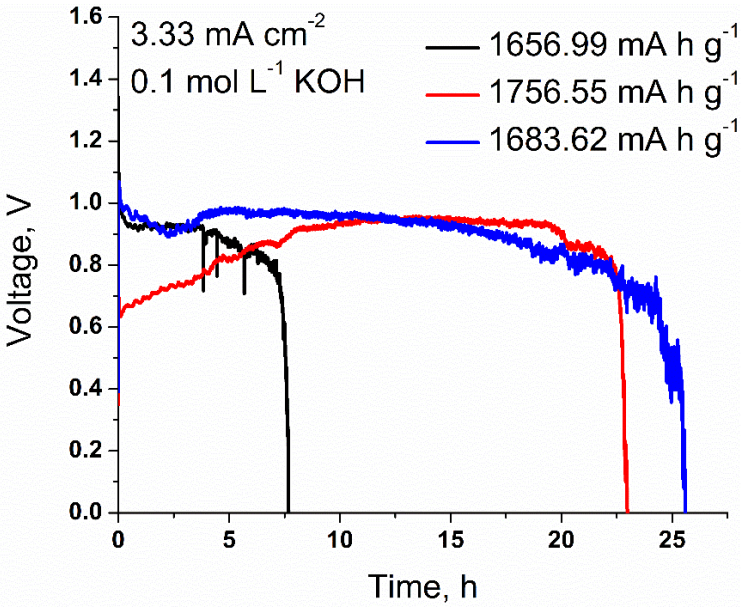

Figure S-12. *Discharge curves and capacity values of the unit cell using aluminum 5052 as anode and 0.1 mol L^{-1} KOH as electrolyte, at current density of 3.33 mA cm^{-2}*

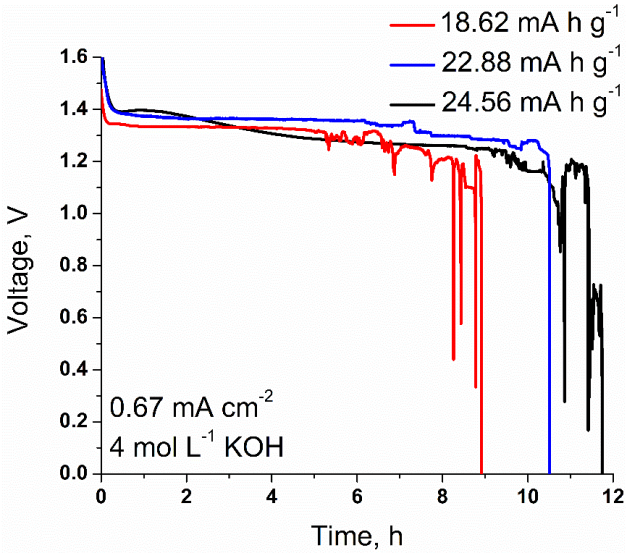

Figure S-13. *Discharge curves and capacity values of the unit cell using aluminum 5052 as anode and 4 mol L $^{-1}$ KOH as electrolyte, at current density of 0.67 mA cm^{-2}*

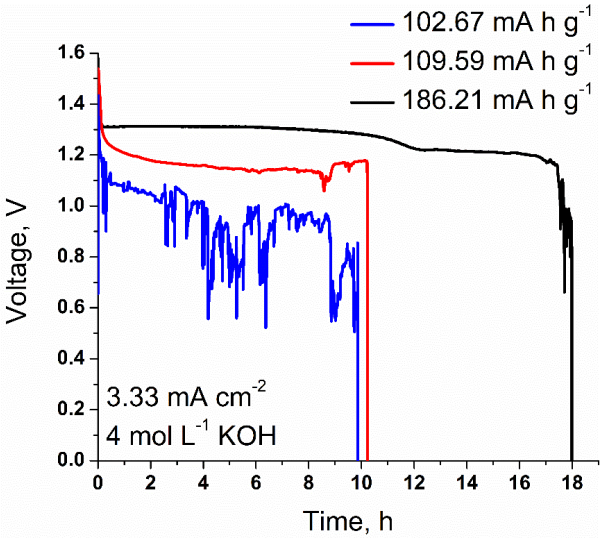

Figure S-14. *Discharge curves and capacity values of the unit cell using aluminum 5052 as anode and 4 mol L^{-1} KOH as electrolyte, at current density of 3.33 mA cm^{-2}*

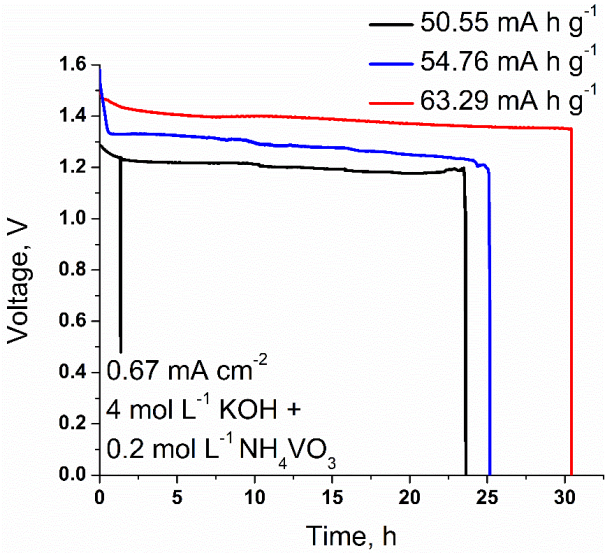

Figure S-15. *Discharge curves and capacity values of the unit cell using aluminum 5052 as anode and 4 mol L^{-1} KOH + 0.2 mol L^{-1} NH_4VO_3 as electrolyte, at current density of 0.67 mA cm^{-2}*

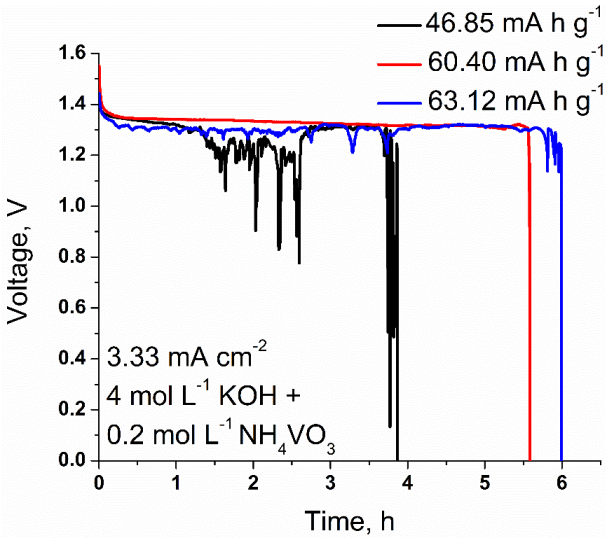

Figure S-16. *Discharge curves and capacity values of the unit cell using aluminum 5052 as anode and 4 mol L^{-1} KOH + 0.2 mol L^{-1} NH_4VO_3 as electrolyte, at current density of 3.33 mA cm^{-2}*

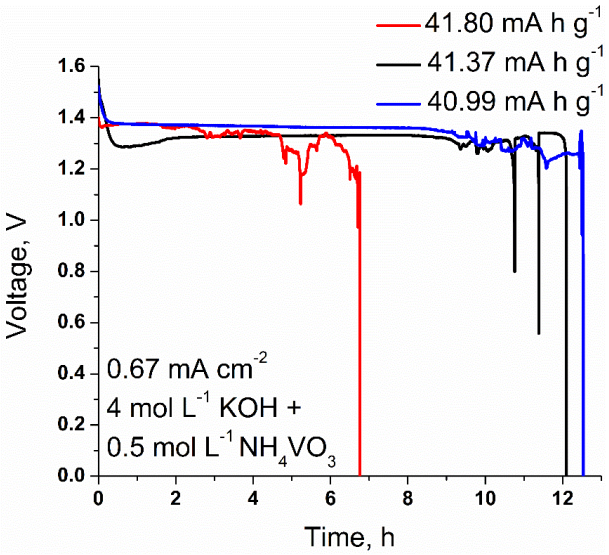

Figure S-17. *Discharge curves and capacity values of the unit cell using aluminum 5052 as anode and 4 mol L^{-1} KOH + 0.5 mol L^{-1} NH_4VO_3 as electrolyte, at current density of 0.67 mA cm^{-2}*

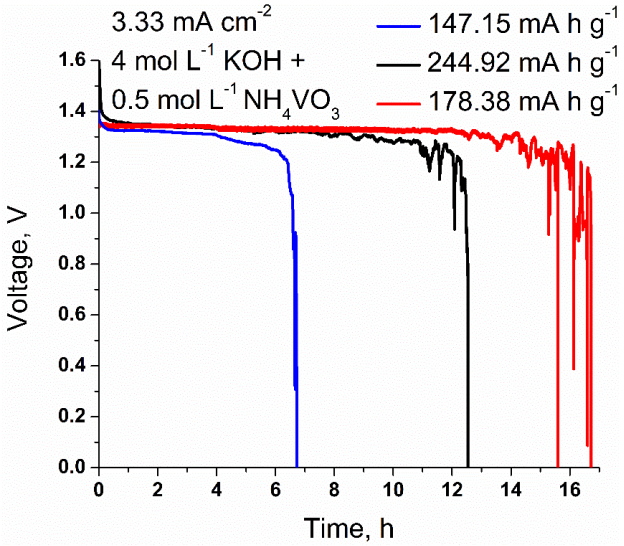

Figure S-18. *Discharge curves and capacity values of the unit cell using aluminum 5052 as anode and 4 mol L^{-1} KOH + 0.5 mol L^{-1} NH_4VO_3 as electrolyte, at current density of 3.33 mA cm^{-2}*

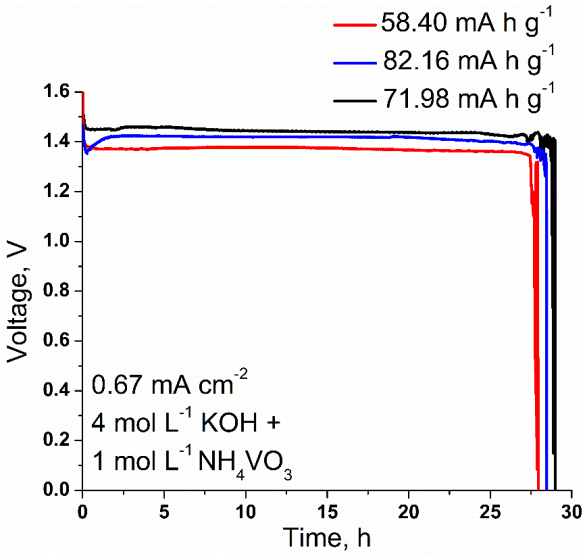

Figure S-19. *Discharge curves and capacity values of the unit cell using aluminum 5052 as anode and 4 mol L^{-1} KOH + 1 mol L^{-1} NH_4VO_3 as electrolyte, at current density of 0.67 mA cm^{-2}*

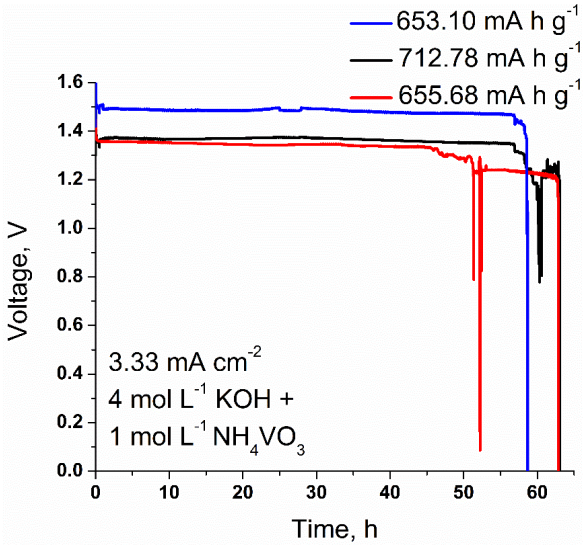

Figure S-20. *Discharge curves and capacity values of the unit cell using aluminum 5052 as anode and 4 mol L^{-1} KOH + 1 mol L^{-1} NH_4VO_3 as electrolyte, at current density of 3.33 mA cm^{-2}*

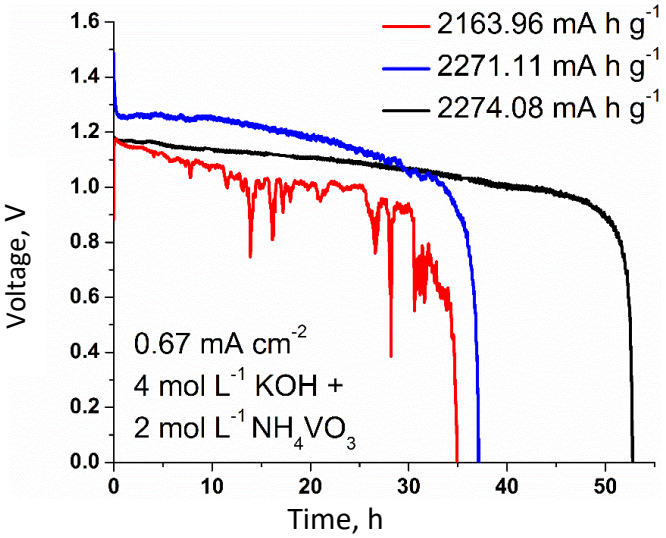

Figure S-21. *Discharge curves and capacity values of the unit cell using aluminum 5052 as anode and 4 mol L^{-1} KOH + 2 mol L^{-1} NH_4VO_3 as electrolyte, at current density of 0.67 mA cm^{-2}*

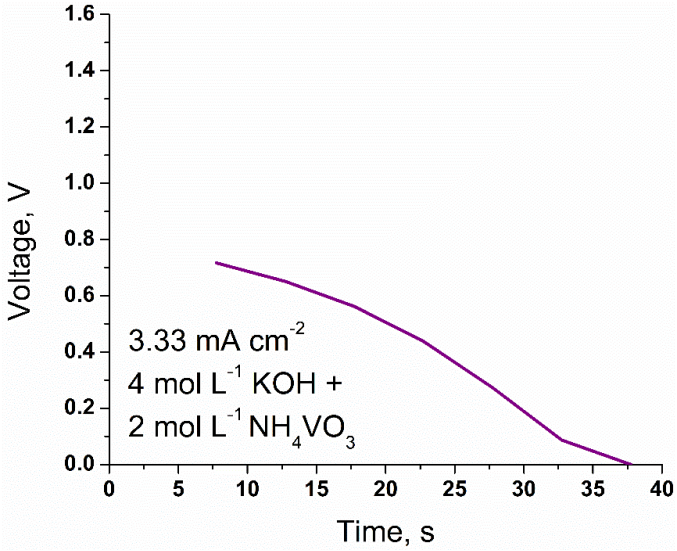

Figure S-22. *Discharge curve of the unit cell using aluminum 5052 as anode and 4 mol L^{-1} KOH + 2 mol L^{-1} NH_4VO_3 as electrolyte, at current density of 3.33 mA cm^{-2}*

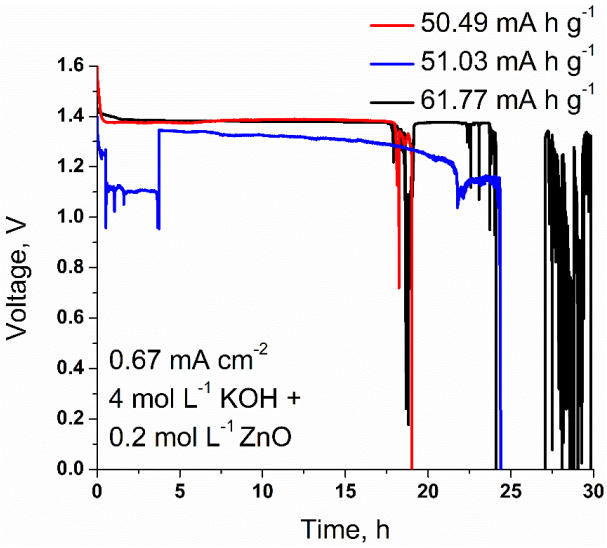

Figure S-23. *Discharge curves and capacity values of the unit cell using aluminum 5052 as anode and 4 mol L^{-1} KOH + 0.2 mol L^{-1} ZnO as electrolyte, at current density of 0.67 mA cm^{-2}*

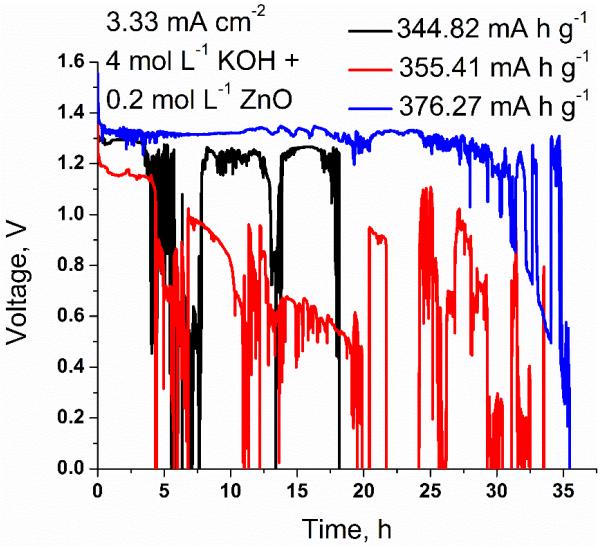

Figure S-24. *Discharge curves and capacity values of the unit cell using aluminum 5052 as anode and 4 mol L^{-1} KOH + 0.2 mol L^{-1} ZnO as electrolyte, at current density of 3.33 mA cm^{-2}*

Figure S-25. *Aluminum 5052 after 100 min of immersion in 4 mol L^{-1} KOH + 0.2 mol L^{-1} ZnO*

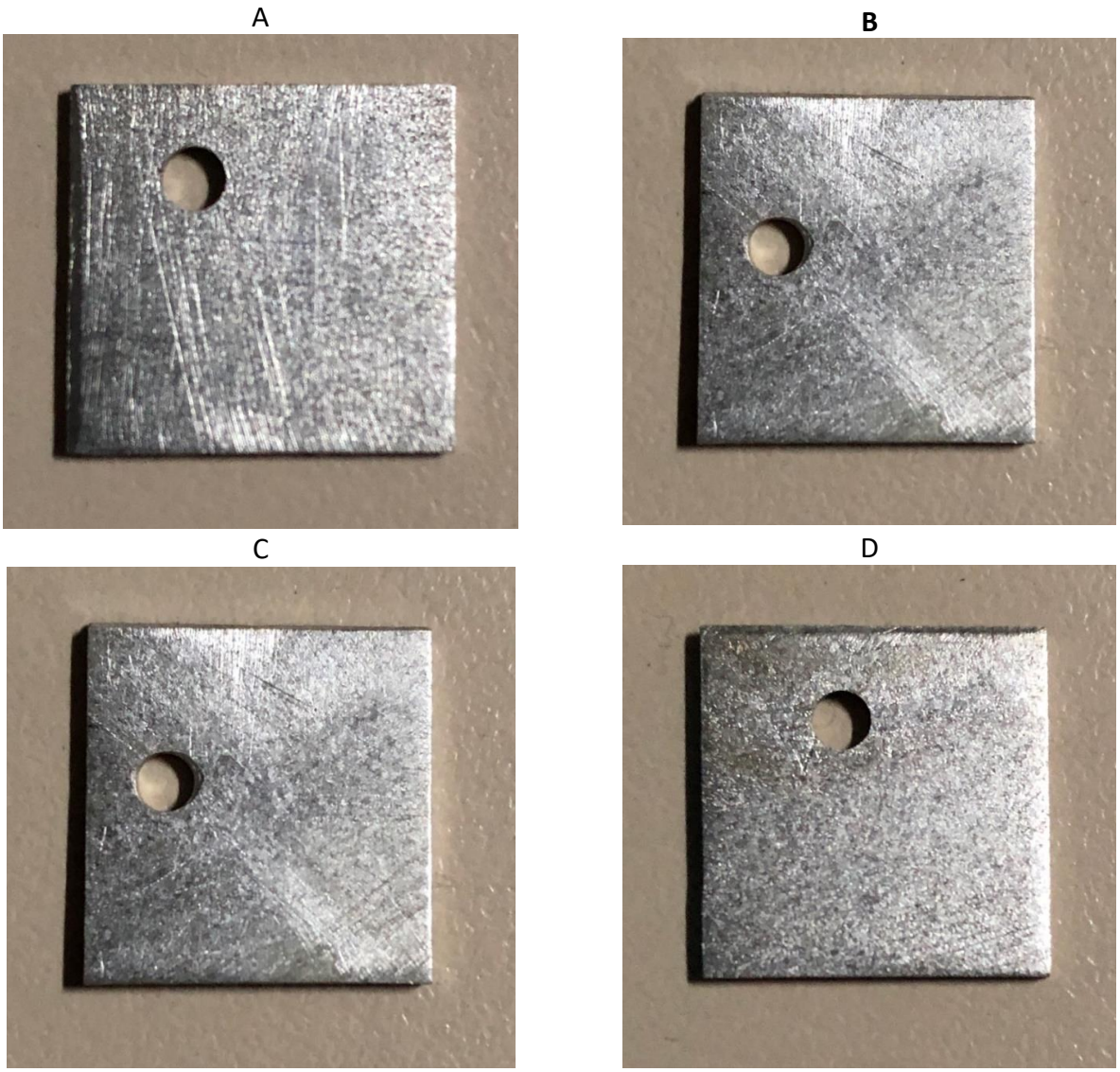

Figure S-26. *Aluminum 5052 after 100 min of immersion in 4 mol L^{-1} KOH + different concentrations of NH_4VO_3: A - 0.2 mol L^{-1}; B – 0.5 mol L^{-1}; C – 1.0 mol L^{-1} and D – 2.0 mol L^{-1}*

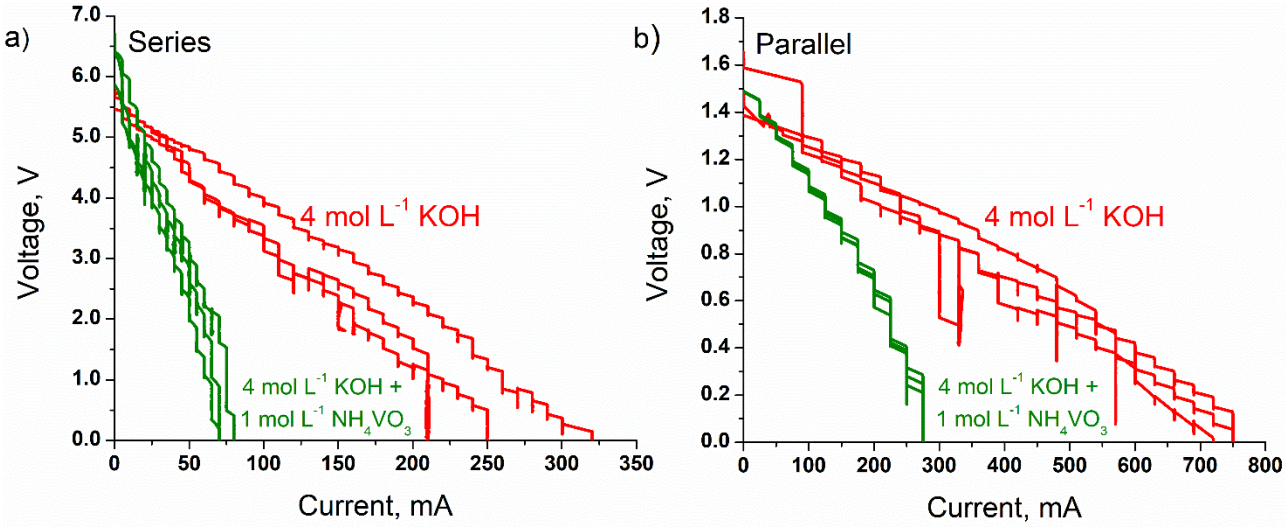

Figure S-27. *Discharge curves of 4-unit-cell arrangement in a) series and b) parallel electrical connection using 4 mol L^{-1} KOH (red) and 4 mol L^{-1} KOH + 1 mol L^{-1} NH_4VO_3 (green) as electrolytes*

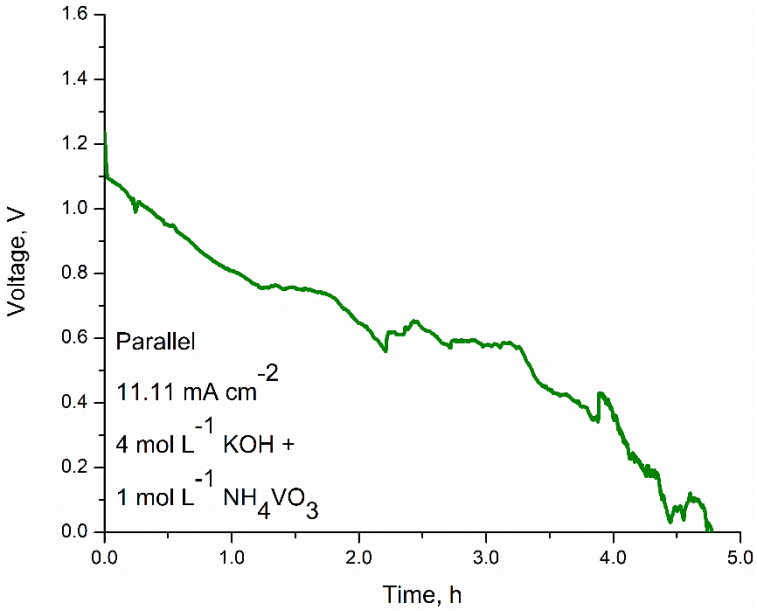

Figure S-28. *Discharge curve obtained with 4-unit cells arranged with electrical connection in parallel using 4 mol L^{-1} KOH + 1 mol L^{-1} NH_4VO_3, at current density of 11.11 mA cm^{-2}*

References

[1] X. Han, X. Li, J. White, C. Zhong, Y. Deng, W. Hu, T. Ma, Metal–Air Batteries: From Static to Flow System, *Advanced Energy Materials* **8** (2018) 1081396. https://doi.org/10.1002/aenm.201801396

[2] S. H. Yang, H. Knickle, Modeling the performance of an aluminum-air cell, *Journal of Power Sources* **124** (2003) 572-585. https://doi.org/10.1016/S0378-7753(03)00811-5